

Hole concentration and phonon renormalization of the 340-cm^{-1} B_{1g} mode in 2% Ca-doped $\text{YBa}_2\text{Cu}_3\text{O}_y$ ($6.76 \leq y \leq 7.00$)

K. C. Hewitt*

Dalhousie University, Department of Physics, Halifax, Nova Scotia, Canada B3H 3J5

X. K. Chen, C. Roch, J. Chrzanowski, and J. C. Irwin

Simon Fraser University, Department of Physics, Burnaby, British Columbia, Canada, V5A 1S6

E. H. Altendorf

Micro Encoder Inc., Kirkland, Washington 98034, USA

R. Liang, D. Bonn, and W. N. Hardy

University of British Columbia, Department of Physics, Vancouver, British Columbia, Canada V6T 1Z1

(Received 7 May 2003; revised manuscript received 7 October 2003; published 27 February 2004)

In order to access the overdoped regime of the $\text{YBa}_2\text{Cu}_3\text{O}_y$ phase diagram, 2% Ca is substituted for Y in $\text{YBa}_2\text{Cu}_3\text{O}_y$ ($y=7.00, 6.93, 6.88, 6.76$). Raman scattering studies have been carried out on these four single crystals. Measurements of the superconductivity-induced renormalization in frequency ($\Delta\omega$) and linewidth ($\Delta 2\gamma$) of the 340-cm^{-1} B_{1g} phonon demonstrate that the magnitude of the renormalization is directly related to the hole concentration p and not simply the oxygen content. The changes in $\Delta\omega$ with p imply that the superconducting gap (Δ_{max}) decreases monotonically with increasing hole concentration in the overdoped regime, and $\Delta\omega$ falls to zero in the underdoped regime. The linewidth renormalization $\Delta 2\gamma$ is negative in the underdoped regime, crossing over at optimal doping to a positive value in the overdoped state.

DOI: 10.1103/PhysRevB.69.064514

PACS number(s): 74.25.Gz, 74.25.Jb, 74.25.Kc, 74.62.Dh

I. INTRODUCTION

Certain phonons in cuprate superconductors exhibit anomalous changes in frequency and linewidth when they are cooled through the superconducting transition temperature. Such phonon anomalies were first discovered in high-temperature superconductors by Macfarlane *et al.*¹ in $\text{YBa}_2\text{Cu}_3\text{O}_{7-\delta}$ (Y123). Zeyher and Zwignagl^{2,3} showed that the presence of such anomalies could be attributed to electron-phonon interactions and the changes in the density of electronic states that occur on the opening of the superconducting gap. Friedl *et al.*⁴ used this approach to obtain an estimate for the superconducting gap in Y-123. Nicol, Jiang and Carbotte⁵ extended the theoretical approach of Zeyher and Zwignagl to include the effect of a pairing interaction of d -wave symmetry on the phonon self-energy. Phonon frequency and linewidth anomalies have been investigated extensively, using Raman scattering, in several cuprates— $\text{YBa}_2\text{Cu}_3\text{O}_{7-\delta}$,^{6–11} $\text{YBa}_2(\text{Cu}_{1-x}\text{M}_x)_4\text{O}_8$ (Y-124) for $\text{M}=\text{Ni}, \text{Zn}$,¹² $\text{Bi}_2\text{Sr}_2\text{CaCu}_2\text{O}_{8+\delta}$ (Bi2212),^{13,14} $\text{NdBa}_2\text{Cu}_3\text{O}_{7-\delta}$ (Nd123),¹⁵ $\text{HgBa}_2\text{Ca}_2\text{Cu}_3\text{O}_{8+\delta}$ (Hg1223),¹⁶ $\text{HgBa}_2\text{Ca}_3\text{Cu}_4\text{O}_{10+\delta}$ (Hg1234),¹⁷ $\text{HgBa}_2\text{Cu}_4\text{O}_{4+\delta}$ (Hg1201),¹⁸ and $(\text{Cu}, \text{C})\text{Ba}_2\text{Ca}_3\text{Cu}_4\text{O}_x$.¹⁹ In particular, many studies have been carried out on the 340-cm^{-1} B_{1g} phonon in Y123 to ascertain the nature of the phonon anomaly. At this time, however, the reason for the sensitivity of the B_{1g} phonon anomaly to extremely small changes in the oxygen content near optimal doping remains somewhat controversial.^{20,21} Additionally, the physical basis of the relationship between hole concentration and the degree of phonon renormalization is unclear, leading some to offer interesting interpretations

based on structural subtleties.²² Anomalies in frequency and linewidth are not the only superconductivity-induced changes. The phonon may also undergo superconductivity-induced changes in intensity and these effects have been studied by a number of groups.^{16,17,19,23–27}

Subsequent to the early experiments^{1,4} it was found^{6,7,28} that the strength of the renormalization is very sensitive to the presence of small amounts of impurities, even in crystals for which the critical temperature remained close to the maximum value of 93.5 K. For example the anomaly is very weak in samples containing a small percentage of either Thorium^{6,7} or Gold,²⁸ where Th substitutes for Yttrium and Au for Cu(1). To explain this effect it was initially suggested that the presence of impurities led to the averaging of an anisotropic gap.²⁹

It was also known³⁰ that the strength of the B_{1g} phonon anomaly is very weak in samples of Y-123 with a reduced oxygen concentration ($y \leq 6.90$), and, in particular,⁹ the strength of the anomaly is very sensitive to oxygen content near optimal doping. For example it is very weak in crystals with $y \leq 6.90$ and $T_c = 92$ K, weak in crystals with $y = 6.95$ and $T_c = 93.7$ K, and yet very strong in overdoped crystals with $y = 7.0$ and $T_c = 89.5$ K. In view of the fact that small changes in oxygen doping produced the same effects as small changes in impurity concentrations it was suggested^{7,9} that the strength of the B_{1g} anomaly is determined by the free carrier, or hole concentration, in the CuO_2 planes. This suggestion was supported by the observation³¹ that the frequency of the pair-breaking peak in the B_{1g} electronic Raman continuum is very sensitive to the level of oxygen doping and, furthermore, that its behavior could be correlated with the strength of the phonon anomaly. That is, the varia-

tion of the frequency of the B_{1g} pair-breaking peak with doping, moved in complete step with the value of the gap obtained from an analysis of the phonon anomaly. The dependence on hole concentration has been questioned in a recent examination of Ca-doped Y-123.³²

In an attempt to gain additional insight into the above question, and into the origin of the physical processes that determine the sensitivity of the B_{1g} phonon anomaly to doping, we have carried out Raman scattering investigations of Ca-doped Y-123 [$Y_{1-x}Ca_xBa_2Cu_3O_y$ or Y(Ca)-123]. Calcium, a divalent alkaline-earth ion, substitutes preferentially for trivalent Yttrium in the $YBa_2Cu_3O_y$ compound. Since the ionic radius of the Ca^{2+} ion is approximately equal to that of the Y^{3+} ion³³ one expects that the carrier or hole concentration could be varied in a controlled manner without introducing any significant distortion in the Y-123 lattice.³⁴ Also, given that the Y-site is located midway between the superconducting CuO_2 planes, Ca substitution should be an effective means of increasing the carrier concentration on the CuO_2 planes. On the basis of simple valence considerations one might thus expect that each substituted Ca ion would contribute 0.5 holes to each CuO_2 plane.^{34,35} Although this recipe appears to break down in the case of more heavily doped samples³⁶ ($x \gtrsim 0.1$), the results presented here, which were obtained using lightly doped ($x=0.02$), high-quality single crystals of Y(Ca)-123, appear to be in accord with these expectations. Our results indicate that the effect of calcium doping on the B_{1g} phonon anomaly is equivalent in every way to the changes induced by appropriate variation of the oxygen concentration. That is, the magnitude of the renormalization is directly related to the hole concentration, in contrast to recent observations.³² In addition, it is found that the superconductivity induced (SCI) frequency renormalization is small for $p < 0.15$, increases rapidly just above optimum doping, and then increases monotonically with increasing hole concentration (for $p > 0.15$). The SCI linewidth renormalization changes from a narrowing below optimal to a broadening above. These results are consistent with the absence of a SCI electronic renormalization in the underdoped state where a pseudogap opens above T_c .

II. SAMPLE PREPARATION & CHARACTERIZATION

Good quality $Y_{1-x}Ca_xBa_2Cu_3O_y$ (Y(Ca)-123) crystals were grown in yttrium-stabilized zirconia crucibles (ZrO_2 -Y) by a standard flux method.³⁷ Based on stoichiometry considerations the [Ca] was estimated to be 4%, but Inductively-Coupled Mass Spectrometry analysis³⁸ yielded a lower value of $2.0 \pm 0.2\%$.

An estimate of the oxygen content (y_{est}) was obtained using the crystal growth parameters of annealing pressure and temperature.³⁹ To determine the values of y more accurately, the c -axis lattice parameter was carefully measured by x-ray diffraction (XRD) studies. Using a Siemens D-5000 diffractometer with $Cu-K_\alpha$ radiation, XRD patterns were obtained using scans with a step size $\Delta\theta = 0.02^\circ$, in the range $5^\circ \leq 2\theta \leq 100^\circ$. In order to obtain reliable estimates of the c -axis lattice parameter only the (00 l) peaks with $2\theta > 30^\circ$ ($l > 5$) were used in a nonlinear least-squares fit to the dif-

TABLE I. Values of the initial oxygen concentration (y_{est}) estimated from the crystal growth parameters. The refined oxygen concentration (y_{ref}) calculated from the c -axis length. p is the hole concentrations calculated from the expression $p = 0.175 - 0.21(7 - y)$ and $p^* = p + [Ca]/2 = p + 0.01$. Crystals A, B, C , and D have $[Ca] = 0.02$, while crystal U is an undoped crystal used for comparison purposes.

Crystal	y_{est}	$c \pm 0.002$ (Å)	y_{ref}	p_{ref}^*	p_{ref}	T_c (K)
A	6.98	11.688	7.00	0.175	0.185	89.5
B	6.95	11.698	6.93	0.161	0.171	92.0
C	6.90	11.707	6.88	0.149	0.159	92.7
D	6.85	11.725	6.76	0.125	0.135	89.5
U	6.95	11.699	6.93	0.160	0.160	93.2

fraction peaks. The refinement program corrects for off-axis shifts and consequently the c -axis spacings reported in Table I are accurate to within ± 0.002 Å.⁴⁰

In agreement with expectations,³⁴ as mentioned above, it was found that the c -axis lattice parameter is not affected by small concentrations of Ca. Therefore, using the relation between the c -axis length and the oxygen concentration,⁹ more accurate values for the oxygen concentrations (y_{ref}) were obtained (see Table I). The samples of 2% Ca-doped Y-123 are therefore labeled according to their oxygen concentration [$y = 7.00(A)$, $6.93(B)$, $6.88(C)$, $6.76(D)$], and an undoped sample [$y = 6.93(U)$] is also used for comparison purposes. The critical temperature T_c was obtained from dc magnetization measurements as described elsewhere.³⁷

The relationship between the oxygen concentration and hole carrier concentration p in the crystals was deduced using a modified form of a relation proposed by Tallon. He proposed that $p = 0.187 - 0.21(7 - y)$, where p is the number of holes per CuO_2 layer and y is the oxygen concentration. In this work, however, we will use a slightly displaced value of the p intercept to be consistent with an optimum hole concentration of 0.16, which is obtained when $y = 6.93$ and $T_{c,max} = 93.7$ K. Accordingly,

$$p = 0.175 - 0.21(7 - y). \quad (1)$$

The critical temperatures of the samples, as a function of the hole concentration per CuO_2 (p), follow the parabolic dependence (Fig. 1) reported in other papers,³⁶

$$T_c/T_{c,max} = 1 - 82.6(p - p_o)^2, \quad (2)$$

where $p_o = 0.16$ is the optimum hole concentration at $T_{c,max}$.

It can be seen from Fig. 1 that crystal C is optimally doped, D is underdoped, and A and B are overdoped. We can conclude that 2% Ca-doping of the Y-123 crystals does not involve any noticeable oxygen depletion, which has been reported^{33,36,41,42} to occur for Ca concentrations greater than 10%. Consequently, the substitution of Calcium (+2) for Yttrium (+3) effectively increases the hole concentration as $p = p^* + [Ca]/2$, where p^* would be the hole concentration in Ca-free material. As one can conclude from an inspection of Table I, only sample A exhibits $y_{est} < y_{ref}$, which may suggest that the sample is oxygen depleted. However,

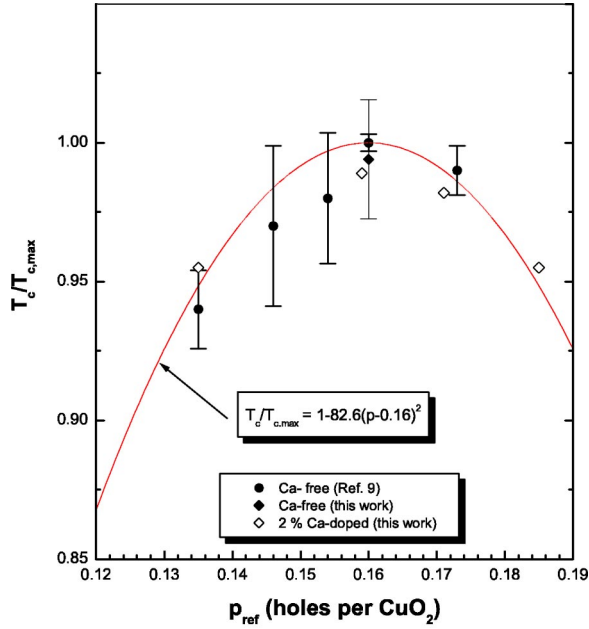


FIG. 1. (Color online) The superconducting transition temperature vs hole concentration for Ca-doped (2%) and Ca-free crystals of Y-123.

since sample *D* is the only underdoped crystal, further investigations are necessary to validate this conclusion.

III. RAMAN SPECTRA

Raman spectra of the Y(Ca)-123 crystals were collected using either the 514.5 nm or 488.0 nm lines of an argon-ion laser as the excitation source. To minimize local heating effects, the incident power was kept below 3 mW, and focussed on the sample with a spherical-cylindrical lens combination to yield incident power densities of the order of 10 W/cm². With this incident power level the local sample heating is minimal. This is clear from the fact that the observed renormalizations occur very close to the measured critical temperatures. Spectra were obtained at various temperatures in the range 15 K < *T* < 300 K, using a Displex refrigerator. All the sample temperatures cited in this paper are the measured ambient temperatures.

Within the *D*_{4h} point group, excitations of *B*_{1g} symmetry are selected by using, in Porto's notation, the *z*(*x'**y'*)*z* scattering geometry, where *x'* denotes the (1,1,0) direction, *y'* denotes the (−1,1,0) direction, and *z* is the direction parallel to the *c* axis. In this geometry the (1,0,0) and (0,1,0) axes lie along the Cu—O bonds. The scattered light was analyzed with a triple-grating spectrometer, using gratings with a bandpass of either 700 cm^{−1} or 1400 cm^{−1}. The corresponding resolution at the detector is 0.8 or 1.6 cm^{−1}, respectively. The scattered light is detected by an ITT-Mepsicon imaging detector over a typical collection time of 1 h. The spectra were carefully calibrated against the laser plasma lines.

*B*_{1g} spectra were obtained at several different temperatures for all samples. Spectra at 16.6 K from sample *A* is

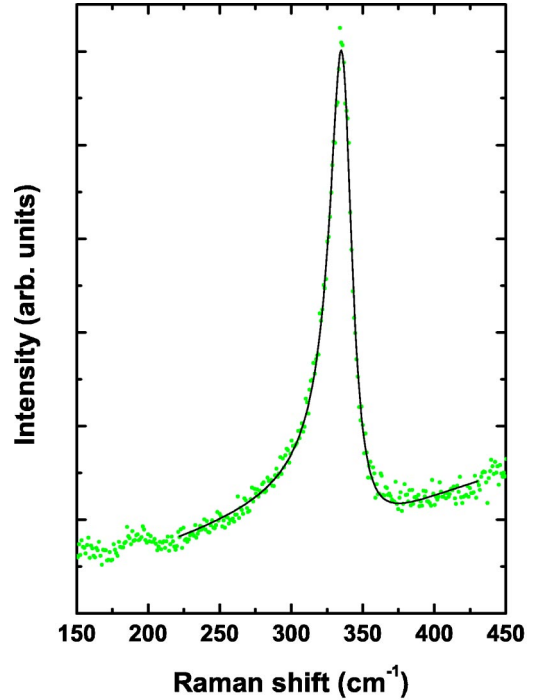


FIG. 2. (Color online) A line shape fit (solid line) to the (nominal) 340-cm^{−1} phonon found in the *B*_{1g} spectra (dots) of sample *A* at *T* = 16.6 K, resulting in $\omega = 336.3 \pm 0.1$ cm^{−1}, $q = -6.0 \pm 0.2$ and HWHM $\gamma = 9.6 \pm 0.1$ cm^{−1}.

shown in Fig. 2. Quantitative analysis of the linewidth ($2\gamma = \Gamma$) and frequency (ω_o) of this mode was carried out by fitting the line shapes to Fano profiles⁴³ with a linear background ($b\omega + c$),

$$I(\omega) = I_o \frac{(q + \epsilon)^2}{1 + \epsilon^2} + b\omega + c, \quad (3)$$

where

$$I_o = \pi \rho_o T_e^2, \quad (4)$$

$$\epsilon = \frac{(\omega - \omega_o)}{\gamma}, \quad (5)$$

$$\gamma = \pi \rho_o V^2, \quad (6)$$

$$q = \frac{T_p}{\pi \rho_o V T_e}. \quad (7)$$

Here we assume a constant density of electronic states over the energy range of interest (ρ_o), *V* measures the interaction between phonon and electronic continuum states, and *T_e*, *T_p* are the matrix elements characterizing Raman-active transitions to the electronic continuum and phonon states, respectively. γ is the half width at half maximum (HWHM) of the line shape and *q* is the asymmetry parameter which determines the form of the line shape, while *b* and *c* are adjustable constants. An example of the results of such a fit is shown in Fig. 2.

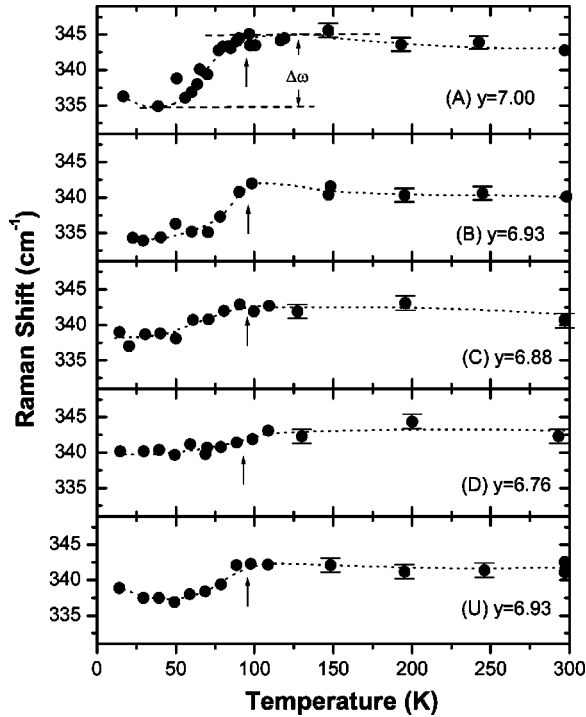


FIG. 3. The temperature dependence of the 340 cm^{-1} phonon frequency, for 2% Ca-doped (A–D) and Ca-free (U) crystals with varying oxygen concentrations.

Friedl *et al.*²⁷ have suggested that intensity anomalies are present because of a superconductivity-induced resonant Raman effect arising from the similar energies of the gap (2Δ) and the phonon ($\hbar\omega_0$). Zhao⁴⁴ carried out similar measurements as a function of doping in $\text{YBa}_2\text{Cu}_3\text{O}_y$ for $y=6.93$ and $y=7.0$ and found that this mechanism, with a d -wave gap, provided a consistent explanation for her data. If the gap energy is much greater than the linewidth, such a resonant effect should not significantly affect the linewidth or frequency of the Raman mode and therefore it is customary to treat the intensity of the phonon profile as a parameter (I_o) in Eq. (3).

The temperature dependence of the frequency (ω_o) and linewidth ($2\gamma = \text{FWHM}$) of the 340-cm^{-1} B_{1g} Raman mode are summarized in Figs. 3 and 4, respectively. As can be seen from these figures, the (nominal) 340-cm^{-1} B_{1g} mode clearly shows significant changes in linewidth and frequency as a function of temperature. In addition, we did not observe significant differences in the frequency and linewidth behavior of the mode when the laser excitation wavelength was switched from 514.5 nm (2.41 eV) to 488.0 nm (2.54 eV). This means that resonance effects, which can alter the redistribution of the Raman continuum⁴⁵ are not important in our case.

As seen in Fig. 3, the magnitude of the phonon frequency decreases substantially in crystals with lower oxygen content. The renormalization is largest⁴⁶ in the highly oxygenated samples and almost vanishes in the sample with an oxygen content $y=6.76$. There is also a substantial softening of the phonon below 100 K; by 11 cm^{-1} in crystals with the highest oxygenation. This softening approximately scales

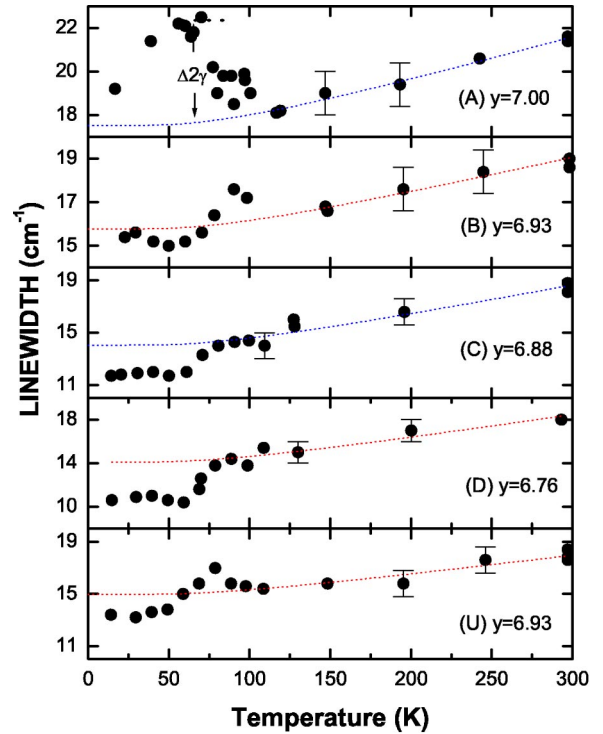


FIG. 4. (Color online) The temperature dependence of the 340-cm^{-1} B_{1g} phonon linewidth for 2% Ca-doped (A–D) and Ca-free (U) crystals with the indicated oxygen concentrations.

with the oxygen content and in crystals with $y=6.76$ the softening is reduced to about $2\text{--}3\text{ cm}^{-1}$.

The linewidth of the 340-cm^{-1} peak (Fig. 4) decreases when cooled between room temperature and 10 K. To determine the superconductivity induced changes one must subtract anharmonic effects. To obtain a rough estimate of the anharmonic changes that occur one can assume that the phonon decays into two phonons with opposite q vector, each having a frequency $\omega_o/2$. The temperature dependence of the linewidth can then be described approximately by the anharmonic decay equation,^{4,47,48}

$$\Gamma_{AH}(\omega_o, T) = c[1 + 2n(\omega_o/2, T)] + d, \quad (8)$$

where n is the Bose-Einstein factor, c and d are constants, and ω_o is the frequency of the mode. Since the Bose factor is approximately constant for temperatures below 100 K (for $\omega_o > 300\text{ cm}^{-1}$), anharmonic effects should be negligible for the 340 cm^{-1} phonon in the range $100\text{ K} > T > 15\text{ K}$. The constants c and d can thus be determined by fitting to the linewidth changes that occur for $T > 100\text{ K}$, and the resulting equation can be used to predict the anharmonic behavior that occurs below 100 K. The superconductivity induced changes are then assumed to be the actual linewidth minus that predicted by the anharmonic equation. These changes are strongly dependent on the oxygen content. In the crystals with very high oxygenation ($y=6.98\text{--}7.00$), there is a pronounced broadening ($\approx 5\text{ cm}^{-1}$ for sample A) of the peak. In samples (C & D) with the lowest oxygen concentration ($y=6.88$ and 6.76), a $2\text{--}3\text{ cm}^{-1}$ steplike narrowing is observed below 80 K without any initial broadening. In the

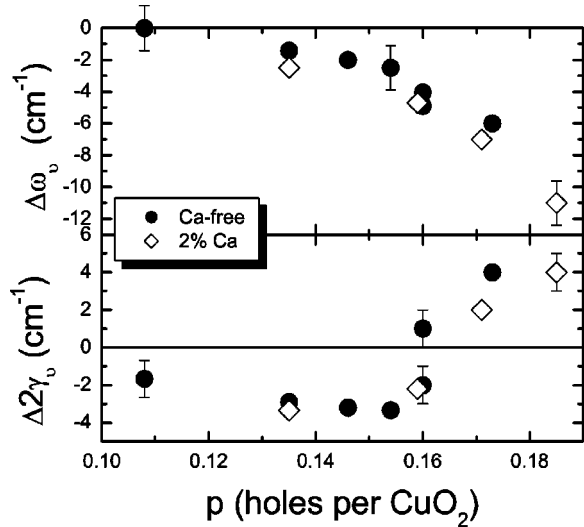


FIG. 5. Superconductivity induced renormalization in frequency and linewidth of the 340-cm^{-1} B_{1g} mode, as a function of hole concentration in Y-123.

crystal (B) possessing an intermediate oxygen content ($y = 6.93$), after an initial broadening (1 cm^{-1}) below 100 K, a narrowing takes place below 50 K (0.5 cm^{-1}).

In order to quantify the SCI changes in frequency and linewidth and to facilitate comparison with the results⁸ obtained from Ca-free crystals, the procedures used in Refs. 4 and 8 will be applied to the results shown in Figs. 3 and 4. That is, the magnitude of the frequency anomaly is estimated by finding the difference in the frequency of the phonon at two temperatures. Quantitatively, for a given doping level, the magnitude of the phonon frequency anomaly ($\Delta\omega$) is determined by the difference in the phonon frequency at 30 K and 100 K,

$$\Delta\omega \equiv \omega(30\text{ K}) - \omega(100\text{ K}).$$

Figure 4 shows that as the sample is cooled below T_c the linewidth departs from the anharmonic decay curve. The phonon linewidth anomaly ($\Delta 2\gamma$) is measured at the temperature T_o ($< T_c$) where the deviation reaches its maximum. It's magnitude is defined as the difference between the linewidth at T_o and the value calculated from anharmonic decay of the phonon at the same temperature,

$$\Delta 2\gamma \equiv 2\gamma(T_o) - \Gamma_{AH}(T_o),$$

where γ_{AH} is the anharmonic linewidth given by Eq. (8).

When $\Delta 2\gamma$ and $\Delta\omega$ are plotted as a function of hole concentration (Fig. 5), a number of features are evident. First, the Ca-free and 2% Ca-doped crystals fall on the same curve. If the [Ca] were ignored, the corresponding points in Fig. 5 would be shifted (by 0.01) to lower hole concentrations, and consequently they would not fall on the same curve as the Ca-free crystals. This observation allows one to conclude that it is the change in hole concentration that is the determining factor— independent of whether it is determined by oxygen or Ca doping.

Second, the most pronounced broadening ($\Delta 2\gamma \approx 5\text{ cm}^{-1}$) and softening ($\Delta\omega = 11\text{ cm}^{-1}$) of the 340 cm^{-1} mode occurs for the sample (A) with the highest hole concentration, estimated to be $p = 0.185$ (Table I). In fact, Fig. 5 demonstrates that the magnitude of the frequency renormalization monotonically increases as the hole concentration is increased. According to theory,^{2,3} as the superconducting gap energy, or the pair-breaking peak in the electronic continuum, approaches the 340 cm^{-1} phonon frequency from above, the phonon damping and frequency renormalization should markedly increase, as is observed. Our results thus imply that for optimal doping, $2\Delta_{max} > \omega_o = 340\text{ cm}^{-1}$, and that the superconducting gap decreases with increasing doping in overdoped crystals. In fact Bock *et al.*,⁴⁹ in thin films with much higher Ca concentrations, carried out measurements on samples with $2\Delta_{max} \leq \omega_o$. They found that $2\Delta_{max} \approx \omega_o$ for a sample with $p \approx 0.20$.

IV. DISCUSSION AND CONCLUSIONS

Substituting Ca for Y in $\text{YBa}_2\text{Cu}_3\text{O}_y$ ($6.85 \leq y < 7$) has allowed us to access the overdoped regime of Y-123. The superconductivity induced renormalization of the 340-cm^{-1} B_{1g} phonon has been studied as a function of oxygen concentration both in pure and in Ca-doped crystals. In overdoped compounds the strength of the phonon anomaly increases as the doping level is increased above optimum ($p = 0.16$). This is consistent with the known behavior of the superconducting gap. In optimally doped compounds the B_{1g} pair breaking peak is centered at $\approx 550\text{ cm}^{-1}$ ($2\Delta_{max} \approx 8.4\text{ kT}$) and this decreases to 470 cm^{-1} ($2\Delta_{max} \approx 7.5\text{ kT}$) for a crystal with $p \approx 0.18$ (Fig. 1). Thus the gap energy is approaching the phonon frequency from above and the increase in strength of the phonon anomaly is consistent with the predictions of Nicol, Jiang, and Carbotte.⁵ The results presented here are consistent with the measurements of Bock *et al.*⁴⁹ carried out on high-quality thin films of Ca-doped Y-123. They also found that the superconducting gap is reduced with increased doping in the overdoped regime. This variation in the gap energy with hole concentration, in the overdoped regime, is very similar to that found in Bi2212 (Ref. 50) and La214.⁵¹ It is clear that the behavior of the superconducting gap in high-quality crystals containing 2% Ca is identical to that observed in undoped samples with the same hole concentration.

As noted above, the frequency shift associated with the phonon anomaly undergoes rather dramatic changes as the doping level moves through optimum. From Fig. 5 one can see that for $p = 0.185$, a doping level slightly above optimum, $\Delta\omega \approx 12\text{ cm}^{-1}$. $\Delta\omega$ then decreases quite rapidly to $\approx 4\text{ cm}^{-1}$ at optimum ($p_o = 0.16$). As the doping level is reduced below optimum $\Delta\omega$ decreases more gradually, and reaches a value ($\approx 2\text{ cm}^{-1}$) that is comparable to the experimental uncertainty when $p \approx 0.14$. On the other hand, the SCI linewidth change ($\Delta 2\gamma$) is even more dramatic in that it abruptly changes from a positive value to a negative value (Fig. 5) as the doping level is reduced through optimum. From Fig. 5 it is clear that crystals with the same hole concentration yield the same phonon anomaly, irrespective of

whether the crystal was doped with Ca or not. This conclusion is in contrast to that presented in Ref. 32 and it is of interest to explore the origin of the discrepancy between the results obtained here and those of Ref. 32. In our opinion these differences primarily involve questions related to the samples used in each study. We have used lightly doped, high-quality single crystals in our work and hence the actual doping level is well known, and a clear and definitive polarization analysis can be carried out. On the other hand the results of Ref. 32 were obtained on relatively heavily doped polycrystalline samples. It is difficult³⁶ to obtain an accurate determination of the doping level in such samples, and furthermore, such samples are more likely to be spatially inhomogeneous. Finally the Raman spectra obtained from such samples are a combination of c axis and in-plane contributions and contain input from all scattering geometries. Separating out the planar B_{1g} response in such samples, to enable a reliable comparison with our data, would be very difficult.

Some workers²² suggest that the electric field produced across a CuO_2 plane by the surrounding asymmetric environment of Y^{3+} and Ba^{2+} is correlated with the strength of the B_{1g} electron-phonon interaction and also the degree of buckling in the CuO_2 plane. Furthermore Chmaissem *et al.*⁵² argued that changes in T_c are directly tied to changes in buckling. It is thus of interest to ask to what degree such factors influence the results presented in this work. For example, does light doping with Ca induce significant distortions or crystal field effects that would compete with effects due to changes in hole concentration? This question is answered by observing that the measured strength of the phonon anomaly in Ca-doped and Ca-free samples, with equal hole concentrations, is the same (Fig. 5), despite the presumed reduction in both the crystal field and buckling due to the substitution of Y^{3+} by Ca^{2+} (substituting Ca^{2+} for Y^{3+} reduces the asymmetry of the environment).²² It is clear from our results that for a given oxygen content (y), doping with Ca increases the strength of the phonon anomaly. Since doping with Ca reduces the charge asymmetry, and hence the electric field across the planes, our results would appear to be inconsistent with the mechanism proposed in Ref. 22. Moreover, Fischer *et al.*³⁴ carried out detailed structural measurements of Ca-doped Y-123. They found that there are no changes in either the c - or a -axis parameters for Ca concentrations in the range $0 \leq x \leq 0.3$, and furthermore, no changes in the b -axis parameter for $0 \leq x \leq 0.1$. These results³⁴ are thus consistent with our observations, and strongly suggest that light doping with Ca does not produce any significant structural distortions in Y-123. Therefore, if buckling, crystal field, and hole concentration are possible causes of the change in the phonon anomaly, our results indicate that it is the hole concentration that provides the dominant, if not sole, contribution.

The addition of calcium might be expected to increase disorder in the crystal and hence might influence the SCI renormalization. One would, *a priori*, predict that at the same hole concentration level, disorder should be greater for the Ca-substituted as compared with the Ca-free samples, all other things being equal. Our results show that the superconductivity-induced phonon renormalization in fre-

quency and linewidth are identical (within experimental error) for all samples with the same doping level (Fig. 5). Thus, the renormalization is independent of any presumed disorder at the 2% Ca doping level. One may of course, introduce disorder by doping Ca at much higher levels, and several workers have done so, but then to extract the effect of disorder and hole doping level would be problematic though some theorists⁵³ have analyzed this problem. For all these reasons we have chosen a low level of doping where we find that disorder does not play a role.

Through its effect on the hole concentration, the addition of calcium could also modify the band structure, Fermi energy, and the Fermi surface shape and, in turn, give rise to resonance effects.⁴⁶ However, these changes are expected to be negligible over the small doping range (0.05 holes about optimal) used in this study, as demonstrated by Angle Resolved Photoemission spectroscopy (ARPES) measurements on $\text{Bi}_2\text{Sr}_2\text{CaCu}_2\text{O}_{8+\delta}$ ⁵⁴ and $\text{YBa}_2\text{Cu}_3\text{O}_y$ ($y = 6.5-6.9$).^{55,56} On the other hand, there are large changes in the density of states (DOS) at the Fermi surface that are associated with the opening of the pseudogap. These DOS changes will have a large effect on T_c and the associated phonon renormalization. Consequently, it is our contention that these changes provide the dominant doping influence on the B_{1g} line profile, and as a result, a consistent explanation for the observed phonon self-energy behavior.

The results shown in Figs. 3–5 suggest that the electron-phonon interaction decreases rapidly as the doping level is reduced through the optimum value. This can be attributed to a corresponding decrease in the carrier concentration, and thus the results are consistent with investigations^{51,57} which show that the pseudogap opens abruptly, and the B_{1g} spectral weight decreases dramatically, as the doping level in Y-123 is reduced below p_o . The absence of a phonon frequency anomaly, and a narrowing of the linewidth, are thus completely consistent with this picture^{51,57,58} of the pseudogap. The results also suggest that Ca doping does not influence the onset of the pseudogap, and again, in high-quality samples, the pseudogap opens at a particular hole concentration, irrespective of how it is generated. Finally, recent theoretical work by Varlamov *et al.*⁵⁹ demonstrates that the pseudogap suppresses the phonon anomaly, providing strong support for the conclusions reached in the present work.

It is also interesting to note that the SCI renormalization of the B_{1g} electronic continuum in Y-123 and La214 vanishes⁵¹ rather abruptly as the doping level is reduced below optimum, and its doping dependence has been found³¹ to be closely correlated with that of the phonon anomaly. This is in contrast to results obtained in Bi2212 (Ref. 50) where it is found that a SCI renormalization of the B_{1g} electronic continuum is observed well into ($p \approx 0.12$) the underdoped region. This result has been attributed to an inherent inhomogeneity^{50,60,61} in Bi2212; that is, in the underdoped material, Bi2212 is composed of underdoped and optimally doped regions. One might speculate that a similar inhomogeneity, due for example to doping variation between grains, might be present in polycrystalline samples of $\text{Y}_{1-x}\text{Ca}_x\text{Ba}_2\text{Cu}_3\text{O}_y$ with $x \geq 0.10$.

In summary, Raman scattering measurements of the

superconductivity-induced renormalization in frequency and linewidth of the 340-cm^{-1} B_{1g} phonon have been completed on single crystals of Ca-doped Y-123. The changes in $\Delta\omega$ with p imply that the superconducting gap (Δ_{max}) decreases monotonically with increasing hole concentration in the overdoped regime, and $\Delta\omega$ falls to zero in the underdoped regime. The linewidth renormalization $\Delta 2\gamma$ is negative in the underdoped regime, crossing over at optimal doping to a positive value in the overdoped state. The measurements

demonstrate that the magnitude of the renormalization is directly related to the hole concentration p , and not simply the oxygen content, or dopant concentration.

ACKNOWLEDGMENT

The financial support of the Natural Sciences and Engineering Research Council of Canada is gratefully acknowledged.

- *Electronic address: Kevin.Hewitt@Dal.ca <http://fizz.phys.dal.ca/~hewitt>
- ¹R.M. Macfarlane, H.J. Rosen, and H. Seki, *Solid State Commun.* **63**, 831 (1987).
 - ²R. Zeyher and G. Zwirgagl, *Solid State Commun.* **66**, 617 (1988).
 - ³R. Zeyher and G. Zwirgagl, *Z. Phys. B: Condens. Matter* **78**, 175 (1990).
 - ⁴B. Friedl, C. Thomsen, and M. Cardona, *Phys. Rev. Lett.* **65**, 915 (1990).
 - ⁵E.J. Nicol, C. Jiang, and J.P. Carbotte, *Phys. Rev. B* **47**, 8131 (1993).
 - ⁶E. Altendorf, J.C. Irwin, W.N. Hardy, and R. Liang, *Physica C* **185-189**, 1375 (1991).
 - ⁷E. Altendorf, J. Chrzanowski, J.C. Irwin, A.O. O'Reilly, and W.N. Hardy, *Physica C* **175**, 47 (1991).
 - ⁸E. Altendorf, J.C. Irwin, R. Liang, and W.N. Hardy, *Phys. Rev. B* **45**, 7551 (1992).
 - ⁹E. Altendorf, X.K. Chen, J.C. Irwin, R. Liang, and W.N. Hardy, *Phys. Rev. B* **47**, 8140 (1993).
 - ¹⁰R. Hauff, S. Tajima, W.J. Jang, and A.I. Rykov, *Phys. Rev. Lett.* **77**, 4620 (1996).
 - ¹¹A.G. Panfilov, M.F. Limonov, A.I. Rykov, S. Tajima, and A. Yamanaka, *Phys. Rev. B* **57**, R5634 (1998).
 - ¹²N. Watanabe and N. Koshizuka, *Phys. Rev. B* **57**, 632 (1998).
 - ¹³D.H. Leach, C. Thomsen, and M. Cardona, *Solid State Commun.* **88**, 457 (1993).
 - ¹⁴A.A. Martin, J.A. Sanjurjo, K.C. Hewitt, X.-Z. Wang, J.C. Irwin, and M.J.G. Lee, *Phys. Rev. B* **56**, 8426 (1997).
 - ¹⁵O.V. Misochko, K. Kuroda, and N. Koshizuka, *Phys. Rev. B* **56**, 9116 (1997).
 - ¹⁶X. Zhou, M. Cardona, D. Colson, and V. Viallet, *Phys. Rev. B* **55**, 12770 (1997).
 - ¹⁷V.G. Hadjiev, X. Zhou, T. Strohm, M. Cardona, Q.M. Lin, and C.W. Chu, *Phys. Rev. B* **58**, 1043 (1998).
 - ¹⁸M.C. Krantz, C. Thomsen, H. Mattausch, and M. Cardona, *Phys. Rev. B* **50**, 1165 (1994).
 - ¹⁹V.G. Hadjiev, M. Cardona, Z.L. Du, Y.Y. Xue, and C.W. Chu, *Phys. Status Solidi B* **205**, R1 (1998).
 - ²⁰A.P. Litvinchuk, C. Thomsen, and M. Cardona, *Solid State Commun.* **83**, 343 (1992).
 - ²¹A.P. Litvinchuk, C. Thomsen, M. Cardona, L. Borjesson, P. Berastegui, and L.-G. Johansson, *Phys. Rev. B* **50**, 1171 (1994).
 - ²²M. Opel, R. Hackl, T.P. Devereaux, A. Virosztek, A. Zawadowski, A. Erb, E. Walker, H. Berger, and L. Forro, *Phys. Rev. B* **60**, 9836 (1999); T.P. Devereaux, A. Virosztek, and A. Zawadowski, *ibid.* **51**, 505 (1995).
 - ²³R. Li, U. Weimer, R. Feile, C. Tomé-Rosa, and H. Adrian, *Physica C* **175**, 89 (1991).
 - ²⁴E.Ya. Sherman, R. Li, and R. Feile, *Phys. Rev. B* **52**, R15757 (1995).
 - ²⁵O.V. Misochko, E.Ya. Sherman, N. Umesaki, K. Sakai, and S. Nakashima, *Phys. Rev. B* **59**, 11 495 (1999).
 - ²⁶E.Ya. Sherman and O.V. Misochko, *Phys. Rev. B* **63**, 104520 (2001).
 - ²⁷B. Friedl, C. Thomsen, H.-U. Habermeier, and M. Cardona, *Solid State Commun.* **78**, 291 (1991).
 - ²⁸K.F. McCarty, J.Z. Liu, Y.X. Jia, R.N. Shelton, and H.B. Radowsky, *Physica C* **192**, 331 (1992).
 - ²⁹C. Thomsen, B. Friedl, M. Cieplak, and M. Cardona, *Solid State Commun.* **78**, 727 (1991).
 - ³⁰M. Krantz, H.J. Rosen, R.M. Macfarlane, and V.Y. Lee, *Phys. Rev. B* **38**, 4992 (1988).
 - ³¹X.K. Chen, E. Altendorf, J.C. Irwin, R. Liang, and W.N. Hardy, *Phys. Rev. B* **48**, 10 530 (1993).
 - ³²J.W. Quilty and H.J. Trodahl, *Phys. Rev. B* **61**, 4238 (2000).
 - ³³C. Greaves and P.R. Slater, *Supercond. Sci. Technol.* **2**, 5 (1989).
 - ³⁴B. Fisher, J. Genossar, C.G. Kuper, L. Patlagan, G.M. Reisner, and A. Knizhnik, *Phys. Rev. B* **47**, 6054 (1993).
 - ³⁵R.A. Gunasekaran, R. Ganguly, and J.V. Yakhmi, *Physica C* **243**, 160 (1995).
 - ³⁶J.T. Kucera and J.C. Bravman, *Phys. Rev. B* **51**, 8582 (1995).
 - ³⁷R. Liang, P. Dosanjh, D.A. Bonn, D.J. Barr, J.F. Carolan, and W.N. Hardy, *Physica C* **195**, 51 (1992).
 - ³⁸Measurements conducted at ALS Environmental, 1988 Triumph Street, Vancouver, BC, Canada V5L 1K5, Tel: 604 253 4188.
 - ³⁹P. Schlegler, W.N. Hardy, and B.X. Yang, *Physica C* **176**, 261 (1991).
 - ⁴⁰J.L. Tallon, C. Bernhard, H. Shaked, R.L. Hitterman, and J.D. Jorgensen, *Phys. Rev. B* **51**, 12911 (1995).
 - ⁴¹A. Manthiram and J.B. Goodenough, *Physica C* **159**, 760 (1989).
 - ⁴²C. Gledel, J.F. Marucco, and B. Touzelin, *Physica C* **165**, 437 (1990).
 - ⁴³M.V. Klein, in *Physical Properties of High Temperature Superconductors*, edited by D.M. Ginsberg (World Scientific, Singapore, 1989), Chap. 4, p.171.
 - ⁴⁴X. Zhao, M.Sc. thesis, Simon Fraser University, Burnaby, BC, 1994.
 - ⁴⁵E.Ya. Sherman, C. Ambrosch-Draxl, and O.V. Misochko, *Phys. Rev. B* **65**, 140510 (2002).
 - ⁴⁶Actually, in the article of Altendorf *et al.* (1993) (Ref. 9), the broadening of the 340 cm^{-1} mode in their most oxygenated sample ($y=7$) is about twice that observed in our sample A ($x=0.02, y=7$). The presence of potassium (K^+) impurities in their sample is, at least, partly responsible, since the substitution

- of monovalent K for trivalent Y or divalent Ba would increase the hole concentration.
- ⁴⁷P.G. Klemens, *Phys. Rev.* **148**, 845 (1966).
- ⁴⁸D.A. Kleinman, *Phys. Rev.* **118**, 118 (1960).
- ⁴⁹A. Bock, S. Ostertun, R. Das Sharma, M. Rubhausen, K.-O. Subke, and C.T. Rieck, *Phys. Rev. B* **60**, 3532 (1999).
- ⁵⁰K.C. Hewitt and J.C. Irwin, *Phys. Rev. B* **66**, 054516 (2002).
- ⁵¹J.C. Irwin, J.G. Naeini, and X.K. Chen, in *Doping Dependence of the Pseudogap in High Temperature Superconductors: A Raman study*, *Studies of High Temperature Superconductors*, edited by A.V. Narlikar (Nova Science, Commack, New York, 1999), Vol. 27/28.
- ⁵²O. Chmaissem, J.D. Jorgenson, S. Short, A. Knizhnik, Y. Eckstein, and H. Shaked, *Nature (London)* **397**, 45 (1999).
- ⁵³O.V. Misochko and E.Ya. Sherman, *Int. J. Mod. Phys. B* **8**, 3371 (1994).
- ⁵⁴H. Ding, M.R. Norman, T. Yokoya, T. Takeuchi, M. Randeria, J.C. Campuzano, T. Takahashi, T. Mochiku, and K. Kadowaki, *Phys. Rev. Lett.* **78**, 2628 (1997).
- ⁵⁵R. Liu, B.W. Veal, A.P. Paulikas, J.W. Downey, H. Shi, C.G. Olson, C. Gu, A.J. Arko, and J.J. Joyce, *Phys. Rev. B* **45**, 5614 (1992).
- ⁵⁶R. Liu, B.W. Veal, A.P. Paulikas, J.W. Downey, P.J. Kostić, S. Fleshler, U. Welp, C.G. Olson, X. Wu, A.J. Arko, and J.J. Joyce, *Phys. Rev. B* **46**, 11056 (1992).
- ⁵⁷X.K. Chen, J.G. Naeini, K.C. Hewitt, J.C. Irwin, R. Liang, and W.N. Hardy, *Phys. Rev. B* **56**, R513 (1997).
- ⁵⁸J.G. Naeini, X.K. Chen, J.C. Irwin, M. Okuya, T. Kimura, and K. Kishio, *Phys. Rev. B* **59**, 9642 (1999).
- ⁵⁹S. Varlamov and G. Seibold, *Phys. Rev. B* **65**, 132504 (2002).
- ⁶⁰C. Howald, P. Fournier, and A. Kapitulnik, *Phys. Rev. B* **64**, 100504 (2001).
- ⁶¹K.M. Lang, V. Mandhavan, J.E. Hoffman, E.W. Hudson, H. Eisaki, S. Uchida, and J.C. Davis, *Nature (London)* **415**, 412 (2002).